NASA Technical Memorandum 85723

XTRAN2L: A PROGRAM FOR SOLVING THE GENERAL-FREQUENCY
UNSTEADY TRANSONIC SMALL DISTURBANCE EQUATION

WOODROW WHITLOW, JR.

NOVEMBER 1983

NASA

National Aeronautics and
Space Administration

Langley Research Center
Hampton, Virginia 23665

XTRAN2L: A PROGRAM FOR SOLVING THE GENERAL-FREQUENCY UNSTEADY TRANSONIC SMALL DISTURBANCE EQUATION

Woodrow Whitlow, Jr.
NASA Langley Research Center
Hampton, VA 23665

Introduction

One of the most widely used programs for transonic unsteady aerodynamic analysis is the LTRAN2 code of Ballhaus and Goorjian.[1] That code is used to solve the low frequency approximation of the transonic small disturbance (TSD) equation. Steady state boundary conditions are used at the airfoil, in the wake, and on the computational boundaries.

Use of the low frequency approximation and steady state airfoil and wake conditions limit the frequency of unsteady motion that can be analyzed with LTRAN2. Houwink and van der Vooren[2] extended the range of applicability of LTRAN2 by adding unsteady terms to the airfoil and wake boundary conditions; the resulting code was termed LTRAN2-NLR. Hessenius and Goorjian[3] added a time derivative term in the downstream far-field condition as well as unsteady airfoil and wake conditions. Their code, LTRAN2-HI, has been validated in the transonic range by a series of comparisons with experimental data.

Although adding unsteady terms to the airfoil and wake boundary conditions extended the range of applicability of LTRAN2, use of the low frequency approximation of the TSD equation still limits its application to relatively low frequency motions. The programs described in references 1-3 use Murman-Cole (M-C) type dependent spatial differencing[4] that admits nonphysical expansion shock waves as part of the computed solutions. Using steady far-field conditions causes disturbances incident on the boundaries to be reflected back into the computational domain. This necessitated placing the computational boundaries far enough from the airfoil that reflected disturbances did not reach the airfoil during the calculations. Having to place the boundaries

far from the airfoil increases the cost of using the programs because the flow field has to be computed at an increased number of grid points.

To remove some of the limitations described above, a new code, XTRAN2L, has been developed at the NASA Langley Research Center. It was developed by modifying LTRAN2-NLR. The M-C differencing was replaced with Engquist-Osher (E-O) monotone differencing.[5-6] E-O differencing does not admit expansion shocks as part of the solution and increases code efficiency by allowing larger time steps to be used in the time-marching solution. The low frequency limitation was removed by adding the capability of solving the complete TSD equation. The final modification that is discussed in the present work is the implementation of nonreflecting far-field boundary conditions that are consistent with the complete equation.

Edwards et al.[7] added the capability of including aeroelastic effects in the time-marching XTRAN2L solutions, and Seidel et al.[8] made an extensive study to determine optimum methods for distributing cartesian grids. The details of those efforts may be found in the cited material.

Unsteady Transonic Small Disturbance Equations

The codes described in references 1-3 are used to solve the low frequency approximation of the transonic small disturbance (TSD) equation

$$A\phi_{xt} = B\phi_{xx} + \phi_{yy}$$
(1)

where ϕ is a disturbance velocity potential normalized by $cU\delta^{2/3}$, c is airfoil chord, δ is airfoil thickness ratio, and U is freestream speed. The spatial coordinates, x and y, and time, t, are normalized by c, $c/\delta^{1/3}$, and ω^{-1}, respectively, where ω is the frequency of unsteady motion. The coefficient $A = 2kM_\infty^2/\delta^{2/3}$ where M_∞ is free-stream Mach number, and the

reduced frequency $k = \omega c/U$. In references 1 and 3,

$B = (1 - M_\infty^2)/\delta^{2/3} - M_\infty^m(\gamma + 1)\phi_x$, where the choice of the exponent

m is arbitrary. Ballhaus and Goorjian made m a function of M_∞ such that the

critical pressure coefficient, C_p^*, predicted by (1) matched the exact

isentropic C_p^*. Hessenius and Goorjian used m = 2 (Spreiter scaling). In

reference 2, $B = (1 - M_\infty^2)/\delta^{2/3} - M_\infty^2(\gamma^* + 1)\phi_x$, where

$\gamma^* = 2 - (2 - \gamma)M_\infty^2$

Solution Algorithm

In the codes described in references 1-3, solutions of (1) are obtained

using the alternating-direction-implicit (ADI) scheme described in reference

9. Solutions are advanced from the nth level in time to level n+1 using the

following two-step procedure

x-sweep:

$$\frac{A}{\Delta t} \delta_x(\tilde{\phi}_{i,j} - \phi_{i,j}^n) = D_x f_{i,j} + \delta_{yy}\phi_{i,j}^n \tag{2a}$$

y-sweep:

$$\frac{A}{\Delta t} \delta_x(\phi_{i,j}^{n+1} - \tilde{\phi}_{i,j}) = \frac{1}{2} \delta_{yy}(\phi_{i,j}^{n+1} - \phi_{i,j}^n) \tag{2b}$$

where $\tilde{\phi}$ is an intermediate level potential. From references 1 and 9,

$$\delta_x\phi = \frac{2}{x_{i+1} - x_{i-1}}(\phi_{i,j} - \phi_{i-1,j})$$

$$\delta_{yy}\phi = \frac{2}{y_{j+1} - y_{j-1}}(\frac{\phi_{i,j+1} - \phi_{i,j}}{y_{j+1} - y_j} - \frac{\phi_{i,j} - \phi_{i,j-1}}{y_j - y_{j-1}})$$

$$f_{i,j} = \frac{1}{2}\left[\frac{1 - M_\infty^2}{\delta^{2/3}} \phi_{x_{i,j}}^n + B_{i,j}^n \tilde{\phi}_{x_{i,j}}\right]$$

$$B_{i,j}^n = \frac{1 - M_\infty^2}{\delta^{2/3}} - M_\infty^m(\gamma + 1)\phi_{x_{i,j}}^n$$

$$B_{i,j}^n = \frac{1 - M_\infty^2}{\delta^{2/3}} - M_\infty^2(\gamma^* + 1)\phi_{x_{i,j}}^n \qquad \text{(LTRAN2-NLR)}$$

$$\phi_{x_{i+1/2,j}} = \frac{\phi_{i+1,j} - \phi_{i,j}}{x_{i+1} - x_i}$$

The mixed difference operator, D_x, is constructed to maintain conservation form. Murman-Cole (M-C) spatial differencing used in LTRAN2, LTRAN2-NLR, and LTRAN2-HI results in the following form for $D_x f_{i,j}$:

$$D_x f_{i,j} = \frac{2}{x_{i+1} - x_{i-1}}[(1-\varepsilon_i)(f_{i+1/2,j} - f_{i-1/2,j}) + \varepsilon_{i-1}(f_{i-1/2,j} - f_{i-3/2,j})] \qquad (3a)$$

$$\varepsilon_i = \begin{cases} 0 & c_{i+1/2,j}^n + c_{i-1/2,j}^n > 0 \\ 1 & c_{i+1/2,j}^n + c_{i-1/2,j}^n < 0 \end{cases} \qquad (3b)$$

It has been shown that M-C differencing allows stable, entropy-violating expansion shocks to be computed as part of the numerical solution.[6,10] Reference 6 also showed that M-C differencing can trigger numerical instabilities that cause large errors in the calculated aerodynamic loads. Such a case was calculated using LTRAN2-NLR for flow over an MBB-A3 airfoil oscillating in pitch about its leading edge at $M_\infty = 0.8$, $k = 0.2$. A time step of $k\Delta t = 1^o$ was used, and the pitching motion was defined by an unsteady angle of attack $\alpha(t) = - 0.5^o + 0.5^o\sin(kt)$. Figure 1a shows that the steady flow field is mixed subsonic/supersonic with a shock wave of moderate strength located at approximately 65 percent chord. Figures 1b-1f show that during the airfoil oscillation an instability is triggered at the lower leading edge that causes the calculations to diverge. When the monotone differencing scheme of Engquist and Osher[5] is used, expansion shocks are not admitted as part of the computed solution, and the calculations remain stable when methods using M-C differencing have begun to diverge.

4

Engquist-Osher Differencing

The Engquist-Osher (E-O) scheme was first used in implicit algorithms by Goorjian and Van Buskirk[6] who tested the method using a modified LTRAN2 code. Similar modifications were made to LTRAN2-NLR at the NASA Langley Research Center. To incorporate the E-O method into the ADI procedure required the following differencing during the x-sweep:

$$\frac{A}{\Delta t}\, \delta_x(\tilde{\phi}_{i,j} - \phi^n_{i,j}) = \overline{D}_x f_{i-1/2,j} + \delta_{yy}\phi^n_{i,j} \tag{4}$$

where

$$\overline{D}_x f_{i-1/2,j} = \overset{\rightarrow}{\Delta}_x \tilde{f}_{i-1/2,j} + \overset{\leftarrow}{\Delta}_x \hat{f}_{i-1/2,j}$$

$$= \frac{2}{x_{i+1} - x_{i-1}}(\tilde{f}_{i+1/2,j} - \tilde{f}_{i-1/2,j} + \hat{f}_{i-1/2,j} - \hat{f}_{i-3/2,j})$$

$$\tilde{f}_{i-1/2,j} = \frac{1}{2}\left[\frac{1 - M^2_\infty}{\delta^{2/3}}\,\tilde{u}_{i-1/2,j} + (\frac{1 - M^2_\infty}{\delta^{2/3}} - M^2_\infty(\gamma^* + 1)\tilde{u}_{i-1/2,j})\overset{\leftarrow}{\delta}_x\tilde{\phi}_{i,j}\right]$$

$$\hat{f}_{i-1/2,j} = \frac{1}{2}\left[\frac{1 - M^2_\infty}{\delta^{2/3}}\,\hat{u}_{i-1/2,j} + (\frac{1 - M^2_\infty}{\delta^{2/3}} - M^2_\infty(\gamma^* + 1)\hat{u}_{i-1/2,j})\overset{\leftarrow}{\delta}_x\tilde{\phi}_{i,j}\right]$$

$$\tilde{u}_{i-1/2,j} = \min(\frac{1 - M^2_\infty}{\delta^{2/3}M^2_\infty(\gamma^* + 1)} , \frac{\phi^n_{i,j} - \phi^n_{i-1,j}}{x_i - x_{i-1}})$$

$$\hat{u}_{i-1/2,j} = \max(\frac{1 - M^2_\infty}{\delta^{2/3}M^2_\infty(\gamma^* + 1)} , \frac{\phi^n_{i,j} - \phi^n_{i-1,j}}{x_i - x_{i-1}})$$

$$\overset{\leftarrow}{\delta}_x\phi_{i,j} = \frac{\phi_{i,j} - \phi_{i-1,j}}{x_i - x_{i-1}}$$

The complete set of difference equations using the monotone differencing for the x-sweep are presented in Appendix A.

To demonstrate the effect of the monotone differencing on numerical stability, the case of the oscillating MBB A-3 airfoil was recalculated. The pressure distributions, Figure 2, show that the numerical solution remained stable for the duration of the calculations. Goorjian and Van Buskirk reported that for some cases, they were able to increase $k\Delta t$ (and hence code efficiency) by factors of up to 10 and still maintain stability.

Algorithm for the Complete TSD Equation

The ability to treat unsteady motions of all frequencies was obtained by adding the capability to solve the complete TSD equation

$$C\phi_{tt} + A\phi_{xt} = B\phi_{xx} + \phi_{yy}$$

where (5)

$$C = \frac{k^2 M^2}{\delta^{2/3}}$$

Solutions for ϕ are advanced from time level n to time level n+1 using the following ADI method of Rizzetta and Chin[11]

x-sweep:

$$\frac{A}{\Delta t} \delta_x(\tilde{\phi}_{i,j} - \phi_{i,j}^n) = D_x f_{i,j} + \delta_{yy}\phi_{i,j}^n \qquad (6a)$$

or

$$\frac{A}{\Delta t} \delta_x(\tilde{\phi}_{i,j} - \phi_{i,j}^n) = \overline{D}_x f_{i,j} + \delta_{yy}\phi_{i,j}^n \qquad (6b)$$

y-sweep:

$$\frac{C}{\Delta t^2}(\phi_{i,j}^{n+1} - 2\phi_{i,j}^n + \phi_{i,j}^{n-1}) + \frac{A}{\Delta t}\delta_x(\phi_{i,j}^{n+1} - \tilde{\phi}_{i,j}) = \frac{1}{2}\delta_{yy}(\phi_{i,j}^{n+1} - \phi_{i,j}^n) \qquad (6c)$$

For the x-sweep, the algorithm is the same as that for the low frequency equation. Including ϕ_{tt} also requires an extra level of computer storage --

6

levels n+1, n, and n-1 versus levels n+1 and n. The difference approximation for the complete TSD equation are presented in Appendix B. Since the x-sweep is unchanged, only the difference equations for the y-sweep are presented.

Nonreflecting Boundary Conditions

The steady state far-field boundary conditions used in LTRAN2 cause disturbances incident on the grid boundaries to be reflected back into the computational domain. Thus, the boundaries had to be placed far away such that reflected disturbances did not reach the airfoil during the calculations and cause errors in the computed solution. Kwak[12] incorporated the nonreflecting far-field boundary conditions of Engquist and Majda[13] into LTRAN2 which allowed a reduction in the physical extent of the computational grid and saved between 10 and 24 percent in computer time. The boundary conditions of reference 13 are not compatible with (5). Nonreflecting far-field boundary conditions that are consistent with the complete TSD equation are presented in this section.

Assuming B to be locally constant, the transformations

$$\xi = \frac{x}{\sqrt{B}}$$

$$\tau = \frac{A}{BD} x + \frac{2}{D} t$$

where

$$D = (4C + \frac{A^2}{B})^{1/2}$$

were used to transform (2) into the wave equation

$$\phi_{\tau\tau} = \phi_{\xi\xi} + \phi_{yy} \tag{7}$$

A nonreflecting far-field condition for (7) is[14]

$$\phi_\tau + \phi_r + \frac{\phi}{2r} = 0 \tag{8}$$

where

$$r^2 = \xi^2 + y^2$$

In untransformed coordinates, (8) becomes

$$\frac{1}{2}\left(-\frac{A}{B}\frac{x}{r} + D\right)\phi_t + \frac{x}{r}\phi_x + \frac{y}{r}\phi_y + \frac{\phi}{2r} = 0 \tag{9}$$

Allowing x to approach $-\infty$ in (9) with y finite, the following first order plane wave condition at the upstream boundary was obtained

$$\frac{1}{2}\left(\frac{A}{B} + \frac{D}{\sqrt{B}}\right)\phi_t - \phi_x = 0 \tag{10}$$

Similarly, letting $x \to +\infty$ with y finite resulted in the downstream condition

$$\frac{1}{2}\left(-\frac{A}{B} + \frac{D}{\sqrt{B}}\right)\phi_t + \phi_x = 0 \tag{11}$$

As $y \to \pm\infty$ with x finite, the following conditions at the top and bottom boundaries were obtained

$$\frac{D}{2}\phi_t \pm \phi_y = 0 \tag{12}$$

where + and - represent the top and bottom boundaries, respectively. Using $\phi = f(r-\tau)$, -- a solution of (7) that represents outgoing waves -- to replace

ϕ_t by $-\frac{2B}{D}\left(\frac{x}{r} - \frac{A}{D}\right)^{-1}\phi_x$, (12) became

$$\frac{BD}{A}\phi_x \pm \phi_y = 0 \tag{13}$$

The boundary conditions in (13) were used in all numerical experiments. The difference equations for (10), (11), and (13) are presented in Appendix C. When C = 0, (10)-(13) reduce to the boundary conditions for the low frequency equation.[12] The nonreflecting boundary conditions are summarized in Figure 3.

One test of the boundary conditions was in the calculation of unsteady forces on an NACA 64A010 airfoil pitching harmonically (about its quarter chord) ±0.25 degrees (^{0}) about a 0^0 mean angle of attack at $M_\infty = 0.825$ and k = 0.5. For the steady flow, an embedded shock wave is located at

8

approximately 62 percent chord. A reference solution was calculated for four cycles of oscillation (360 steps per cycle) on a 113 x 97 grid (in x,y) that extended 200c in x and 709c in y. The grid was reduced to 88 x 65 ($-3.8c \leq x \leq 3.5c$, $y \leq 9.3c$), and the calculations were made first using steady-state far-field boundary conditions and then using (10), (11), and (13) at the boundaries. As shown in Figure 4, when the steady conditions were used, disturbances reflected from the boundaries caused the calculated lift to deviate significantly from the large grid value. When the nonreflecting boundary conditions were implemented, most of the waves incident on the boundaries were absorbed, and the small grid results showed good agreement with the reference calculation. Those results are also shown in Figure 4. Compared with the time required to generate the large grid solution (3215 seconds on a CDC CYBER 173), using the new boundary conditions on the small grid resulted in a 44 percent savings in computer time (the small grid solution required 1815 seconds).

A second test was to calculate the unsteady force response for a flat plate airfoil with a pulse in angle of attack α. The calculations were made for $M_\infty = 0.85$ on an 80 x 61 grid that extended $\pm 20c$ in x and $\pm 25c$ in y. Using the pulse/transfer function technique described in Reference 8, the frequency response function for the unsteady lift curve slope c_{ℓ_α} was calculated with and without the nonreflecting boundary conditions. In the pulse/transfer function technique, after α was increased smoothly and rapidly to a maximum and returned to its initial value, calculation of the unsteady forces were continued until those forces returned to their starting values. A Fast Fourier Transform (FFT) of the lift coefficient c_ℓ was then divided by the α FFT to obtain the frequency response function for c_{ℓ_α}. A flat plate airfoil was used to allow comparisons of the forces calculated using XTRAN2L with those predicted using the exact kernel function method of Bland.[15]

Figure 5a shows a comparison of the unsteady forces calculated using steady state conditions on the computational boundaries with the forces obtained using Bland's kernel function method. Below k ≈ 0.5, the finite difference results have spurious oscillations due to disturbances reflected from the boundaries. When the nonreflecting boundary conditions were used (Figure 5b), the reflected disturbances were small, and good agreement with the exact solution was obtained.

Concluding Remarks

A new computer program, XTRAN2L, for transonic unsteady aerodynamic analysis has been developed at the NASA Langley Research Center. It is a modification of the LTRAN2-NLR code. The monotone differencing method of Engquist and Osher was used to replace the Murman-Cole type dependent differencing scheme. That resulted in a code that is more robust and more efficient, and the new differencing method does not admit nonphysical expansion shocks as part of computed solutions. The capability of analyzing airfoils undergoing motions of all frequencies was obtained by adding a general frequency term to the transonic small disturbance (TSD) equation. Solutions of the complete TSD equation are advanced through time using the alternating-direction-implicit method of Rizzetta and Chin. Nonreflecting boundary conditions that reduced disturbances reflected from the computational boundaries were implemented. This allowed the boundaries to be moved closer to the airfoil and thus further increased program efficiency.

APPENDIX A

DIFFERENCE EQUATION FOR THE ENGQUIST-OSHER METHOD

The difference equation that results when Engquist-Osher (E-O) monotone differencing is used in the x-sweep of the solution procedure is presented in this Appendix. When the E-O method is used, the finite difference approximation of (4) becomes

$$
\frac{A}{\Delta t} \left(\tilde{\phi}_{i,j} - \tilde{\phi}_{i-1,j} - \phi^n_{i,j} + \phi^n_{i-1,j} \right) =
$$

$$
\frac{1}{2} \frac{1 - M^2_\infty}{\delta^{2/3}} \min \left(\overline{u}, \frac{\phi^n_{i+1,j} - \phi^n_{i,j}}{x_{i+1} - x_i} \right) +
$$

$$
\frac{1}{2} \left[\frac{1 - M^2_\infty}{\delta^{2/3}} - M^2_\infty (\gamma^* + 1) \min \left(\overline{u}, \frac{\phi^n_{i+1,j} - \phi^n_{i,j}}{x_{i+1} - x_i} \right) \right] \frac{\tilde{\phi}_{i+1,j} - \tilde{\phi}_{i,j}}{x_{i+1} - x_i}
$$

$$
- \frac{1}{2} \frac{1 - M^2_\infty}{\delta^{2/3}} \min \left(\overline{u}, \frac{\phi^n_{i,j} - \phi^n_{i-1,j}}{x_i - x_{i-1}} \right) -
$$

$$
\frac{1}{2} \left[\frac{1 - M^2_\infty}{\delta^{2/3}} - M^2_\infty (\gamma^* + 1) \min \left(\overline{u}, \frac{\phi^n_{i,j} - \phi^n_{i-1,j}}{x_i - x_{i-1}} \right) \right] \frac{\tilde{\phi}_{i,j} - \tilde{\phi}_{i-1,j}}{x_i - x_{i-1}}
$$

$$
+ \frac{1}{2} \frac{1 - M^2_\infty}{\delta^{2/3}} \max \left(\overline{u}, \frac{\phi^n_{i,j} - \phi^n_{i-1,j}}{x_i - x_{i-1}} \right) +
$$

$$
\frac{1}{2} \left[\frac{1 - M^2_\infty}{\delta^{2/3}} - M^2_\infty (\gamma^* + 1) \max \left(\overline{u}, \frac{\phi^n_{i,j} - \phi^n_{i-1,j}}{x_i - x_{i-1}} \right) \right] \frac{\tilde{\phi}_{i,j} - \tilde{\phi}_{i-1,j}}{x_i - x_{i-1}}
$$

$$
- \frac{1}{2} \frac{1 - M^2_\infty}{\delta^{2/3}} \max \left(\overline{u}, \frac{\phi^n_{i-1,j} - \phi^n_{i-2,j}}{x_{i-1} - x_{i-2}} \right) -
$$

$$
\frac{1}{2} \left[\frac{1 - M^2_\infty}{\delta^{2/3}} - M^2_\infty (\gamma^* + 1) \max \left(\overline{u}, \frac{\phi^n_{i-1,j} - \phi^n_{i-2,j}}{x_{i-1} - x_{i-2}} \right) \right] \frac{\tilde{\phi}_{i-1,j} - \tilde{\phi}_{i-2,j}}{x_{i-1} - x_{i-2}}
$$

$$+ \frac{x_{i+1} - x_{i-1}}{y_{j+1} - y_{j-1}} \left(\frac{\phi^n_{i,j+1} - \phi^n_{i,j}}{y_{j+1} - y_j} - \frac{\phi^n_{i,j} - \phi^n_{i,j-1}}{y_j - y_{j-1}} \right) \tag{A1}$$

where

$$\overline{u} = \frac{1 - M_\infty^2}{\delta^{2/3} M_\infty^2 (\gamma^* + 1)}$$

In the quadradiagonal form

$$A_i \tilde{\phi}_{i-2,j} + B_i \tilde{\phi}_{i-1,j} + C_i \tilde{\phi}_{i,j} + D_i \tilde{\phi}_{i+1,j} = E_i \tag{A2}$$

$$A_i = -\frac{1}{2} \left[\frac{1 - M_\infty^2}{\delta^{2/3}} - M_\infty^2(\gamma^* + 1)\max\left(\overline{u}, \frac{\phi^n_{i-1,j} - \phi^n_{i-2,j}}{x_{i-1} - x_{i-2}}\right) \right] \frac{1}{x_{i-1} - x_{i-2}}$$

$$B_i = -\frac{1}{2} \left[\frac{1 - M_\infty^2}{\delta^{2/3}} - M_\infty^2(\gamma^* + 1)\min\left(\overline{u}, \frac{\phi^n_{i,j} - \phi^n_{i-1,j}}{x_i - x_{i-1}}\right) \right] \frac{1}{x_i - x_{i-1}}$$

$$+ \frac{1}{2} \left[\frac{1 - M_\infty^2}{\delta^{2/3}} - M_\infty^2(\gamma^* + 1)\max\left(\overline{u}, \frac{\phi^n_{i,j} - \phi^n_{i-1,j}}{x_i - x_{i-1}}\right) \right] \frac{1}{x_i - x_{i-1}}$$

$$+ \frac{1}{2} \left[\frac{1 - M_\infty^2}{\delta^{2/3}} - M_\infty^2(\gamma^* + 1)\max\left(\overline{u}, \frac{\phi^n_{i-1,j} - \phi^n_{i-2,j}}{x_{i-1} - x_{i-2}}\right) \right] \frac{1}{x_{i-1} - x_{i-2}} - \frac{A}{\Delta t}$$

$$C_i = \frac{1}{2} \left[\frac{1 - M_\infty^2}{\delta^{2/3}} - M_\infty^2(\gamma^* + 1)\min\left(\overline{u}, \frac{\phi^n_{i+1,j} - \phi^n_{i,j}}{x_{i+1} - x_i}\right) \right] \frac{1}{x_{i+1} - x_i}$$

$$+ \frac{1}{2} \left[\frac{1 - M_\infty^2}{\delta^{2/3}} - M_\infty^2(\gamma^* + 1)\min\left(\overline{u}, \frac{\phi^n_{i,j} - \phi^n_{i-1,j}}{x_i - x_{i-1}}\right) \right] \frac{1}{x_i - x_{i-1}}$$

$$- \frac{1}{2} \left[\frac{1 - M_\infty^2}{\delta^{2/3}} - M_\infty^2(\gamma^* + 1)\max\left(\overline{u}, \frac{\phi^n_{i,j} - \phi^n_{i-1,j}}{x_i - x_{i-1}}\right) \right] \frac{1}{x_i - x_{i-1}} + \frac{A}{\Delta t}$$

$$D_i = -\frac{1}{2}\left\lfloor\frac{1 - M_\infty^2}{\delta^{2/3}} - M_\infty^2(\gamma^* + 1)\min\left(\overline{u}, \frac{\phi_{i+1,j}^n - \phi_{i,j}^n}{x_{i+1} - x_i}\right)\right\rfloor\frac{1}{x_{i+1} - x_i}$$

$$\begin{aligned}
E_i = &\frac{1 - M_\infty^2}{2\delta^{2/3}}\left\lfloor\min\left(\overline{u}, \frac{\phi_{i+1,j}^n - \phi_{i,j}^n}{x_{i+1} - x_i}\right) - \min\left(\overline{u}, \frac{\phi_{i,j}^n - \phi_{i-1,j}^n}{x_i - x_{i-1}}\right)\right. \\
&\left. + \max\left(\overline{u}, \frac{\phi_{i,j}^n - \phi_{i-1,j}^n}{x_i - x_{i-1}}\right) - \max\left(\overline{u}, \frac{\phi_{i-1,j}^n - \phi_{i-2,j}^n}{x_{i-1} - x_{i-2}}\right)\right\rfloor \\
&+ \frac{A}{\Delta t}(\phi_{i,j}^n - \phi_{i-1,j}^n) + \frac{x_{i+1} - x_{i-1}}{y_{j+1} - y_{j-1}}\left(\frac{\phi_{i,j+1}^n - \phi_{i,j}^n}{y_{j+1} - y_j} - \frac{\phi_{i,j}^n - \phi_{i,j-1}^n}{y_j - y_{j-1}}\right)
\end{aligned}$$

The difference equation for the y-sweep is unchanged.

DIFFERENCE EQUATIONS FOR THE COMPLETE TRANSONIC SMALL DISTURBANCE EQUATION

The difference equations for the complete transonic small disturbance (TSD) equation are discussed in this Appendix. Since the numerical procedure for the x-sweep is the same for the low frequency and the complete TSD equations, only the difference equation for the y-sweep (6c) is presented here. That equation is

$$\frac{C}{\Delta t^2}(\phi_{i,j}^{n+1} - 2\phi_{i,j}^{n} + \phi_{i,j}^{n-1}) + \frac{2A}{\Delta t(x_{i+1} - x_{i-1})}(\phi_{i,j}^{n+1} - \phi_{i-1,j}^{n+1} - \phi_{i,j}^{n} + \phi_{i-1,j}^{n}) =$$

$$\frac{1}{y_{j+1} - y_{j-1}}(\frac{\phi_{i,j+1}^{n+1} - \phi_{i,j}^{n+1}}{y_{j+1} - y_j} - \frac{\phi_{i,j}^{n+1} - \phi_{i,j-1}^{n+1}}{y_j - y_{j-1}} - \frac{\phi_{i,j+1}^{n} - \phi_{i,j}^{n}}{y_{j+1} - y_j} + \frac{\phi_{i,j}^{n} - \phi_{i,j-1}^{n}}{y_j - y_{j-1}}) \quad (B1)$$

In tridiagonal form

$$A_j\phi_{i,j-1}^{n+1} + B_j\phi_{i,j}^{n+1} + C_j\phi_{i,j+1}^{n+1} = D_j \quad\quad (B2)$$

$$A_j = \frac{1}{(y_{j+1} - y_{j-1})(y_j - y_{j-1})}$$

$$B_j = \frac{1}{y_{j+1} - y_{j-1}}(\frac{1}{y_{j+1} - y_j} + \frac{1}{y_j - y_{j-1}}) + \frac{2A}{\Delta t(x_{i+1} - x_{i-1})} + \frac{C}{\Delta t^2}$$

$$C_j = -\frac{1}{(y_{j+1} - y_{j-1})(y_{j+1} - y_j)}$$

$$D_j = -\frac{1}{y_{j+1} - y_{j-1}}(\frac{\phi_{i,j+1}^{n} - \phi_{i,j}^{n}}{y_{j+1} - y_j} - \frac{\phi_{i,j}^{n} - \phi_{i,j-1}^{n}}{y_j - y_{j-1}})$$

$$+ \frac{2A}{\Delta t(x_{i+1} - x_{i-1})}(\phi_{i-1,j}^{n+1} - \phi_{i,j}^{n} + \phi_{i-1,j}^{n}) + \frac{C}{\Delta t^2}(2\phi_{i,j}^{n} - \phi_{i,j}^{n-1})$$

The tridiagonal coefficients are the same as for the low frequency equation with the exception of the $\frac{C}{\Delta t^2}$ term added to B_j and the $\frac{C}{\Delta t^2}(2\phi_{i,j}^{n} - \phi_{i,j}^{n-1})$ term added to D_j.

APPENDIX C

DIFFERENCE EQUATIONS FOR THE NONREFLECTING BOUNDARY CONDITIONS

The difference equations for the nonreflecting boundary conditions are presented in this Appendix. The upstream and downstream boundary conditions are implemented during the x-sweep of the ADI procedure. They are applied midway between the extreme and adjacent grid columns at a time level halfway between level n and the intermediate level at which $\tilde{\phi}$ is defined (n+1/2). At the upstream boundary, i = 1, the plane wave condition is

$$(\tilde{\phi}_t)_{i+1/2,j}^{n+1/2} - b_{i+1/2,j}(\tilde{\phi}_x)_{i+1/2,j}^{n+1/2} = 0 \tag{C1}$$

where

$$b_{i+1/2,j} = \frac{2B_{i+1/2,j}}{A + \left[A^2 + 4B_{i+1/2,j}C\right]^{1/2}}$$

$$B_{i+1/2,j} = \frac{1 - M_\infty^2}{\delta^{2/3}} - M_\infty^2(\gamma^* + 1)\frac{\phi_{i+1,j}^n - \phi_{i,j}^n}{x_{i+1} - x_i}$$

Using centered space and time differences and the relationships

$$\phi_{i\pm1/2,j} = \frac{\phi_{i,j} + \phi_{i\pm1,j}}{2} \tag{C2}$$

$$\phi^{n+1/2} = \frac{\tilde{\phi} + \phi^n}{2} \tag{C3}$$

the difference equation for (C1) becomes

$$\frac{\tilde{\phi}_{i+1,j} + \tilde{\phi}_{i,j} - \phi_{i+1,j}^n - \phi_{i,j}^n}{2\Delta t} - \frac{b_{i+1/2,j}}{2(x_{i+1}-x_i)}(\tilde{\phi}_{i+1,j} - \tilde{\phi}_{i,j} + \phi_{i+1,j}^n - \phi_{i,j}^n) = 0 \tag{C4}$$

In quadradiagonal form

$$A_i\tilde{\phi}_{i-2,j} + B_i\tilde{\phi}_{i-1,j} + C_i\tilde{\phi}_{i,j} + D_i\tilde{\phi}_{i+1,j} = E_i \tag{C5}$$

$$A_i = 0$$

$$B_i = 0$$

$$C_i = 1 + b_{i+1/2,j}\frac{\Delta t}{x_{i+1} - x_i}$$

$$D_i = 1 - b_{i+1/2,j} \frac{\Delta t}{x_{i+1} - x_i}$$

$$E_i = \phi^n_{i+1,j} + \phi^n_{i,j} + b_{i+1/2,j} \frac{\Delta t}{x_{i+1} - x_i}(\phi^n_{i+1,j} - \phi^n_{i,j})$$

At the downstream boundary, i = IMAX (the maximum streamwise grid location), the nonreflecting condition is

$$(\tilde{\phi}_t)^{n+1/2}_{i-1/2,j} + b^*_{i-1/2,j}(\tilde{\phi}_x)^{n+1/2}_{i-1/2,j} = 0 \qquad \text{(C6)}$$

where

$$b^*_{i-1/2,j} = \frac{2B_{i-1/2,j}}{-A + \left| A^2 + 4B_{i-1/2,j}C \right|^{1/2}}$$

$$B_{i-1/2,j} = \frac{1 - M_\infty^2}{\delta^{2/3}} - M_\infty^2(\gamma^* + 1)\frac{\phi^n_{i,j} - \phi^n_{i-1,j}}{x_i - x_{i-1}}$$

In difference form, the downstream condition becomes

$$\frac{\tilde{\phi}_{i,j} + \tilde{\phi}_{i-1,j} - \phi^n_{i,j} - \phi^n_{i-1,j}}{2\Delta t} + \frac{b^*_{i-1/2,j}}{2(x_i - x_{i-1})}(\tilde{\phi}_{i,j} - \tilde{\phi}_{i-1,j} + \phi^n_{i,j} - \phi^n_{i-1,j}) = 0 \qquad \text{(C7)}$$

The quadradiagonal coefficients are

$$A_i = 0$$

$$B_i = 1 - b^*_{i-1/2,j} \frac{\Delta t}{x_i - x_{i-1}}$$

$$C_i = 1 + b^*_{i-1/2,j} \frac{\Delta t}{x_i - x_{i-1}}$$

$$D_i = 0$$

$$E_i = \phi_{i,j}^n + \phi_{i-1,j}^n - b_{i-1/2,j}^* \frac{\Delta t}{x_i - x_{i-1}}(\phi_{i,j}^n - \phi_{i-1,j}^n)$$

At the lower boundary, $j = 1$, the boundary condition that is imposed is

$$(\phi_y)_{i-1/2,j+1/2}^{n+1/2} - a_{i-1/2,j+1/2}(\phi_x)_{i-1/2,j+1/2}^{n+1/2} = 0 \tag{C8}$$

where

$$a_{i-1/2,j+1/2} = \frac{(BD)_{i-1/2,j+1/2}}{A}$$

$$B_{i-1/2,j+1/2} = \frac{1 - M_\infty^2}{\delta^{2/3}} - M_\infty^2 \frac{(\gamma^* + 1)}{2}(\phi_{i,j}^n - \phi_{i-1,j}^n + \phi_{i,j+1}^n - \phi_{i-1,j+1}^n)$$

In tridiagonal form

$$A_j \phi_{i,j-1}^{n+1} + B_j \phi_{i,j}^{n+1} + C_j \phi_{i,j+1}^{n+1} = D_j \tag{C9}$$

the coefficients at the lower boundary are

$$A_j = 0$$

$$B_j = \frac{a_{i-1/2j,+1/2}}{x_i - x_{i-1}} + \frac{1}{y_{j+1} - y_j}$$

$$C_j = \frac{a_{i-1/2,j+1/2}}{x_i - x_{i-1}} - \frac{1}{y_{j+1} - y_j}$$

$$D_j = \frac{\phi_{i-1,j+1}^{n+1} + \phi_{i-1,j+1}^n + \phi_{i,j+1}^n - \phi_{i-1,j}^{n+1} - \phi_{i-1,j}^n - \phi_{i,j}^n}{y_{j+1} - y_j}$$

$$- \frac{a_{i-1/2,j+1/2}}{x_i - x_{i-1}}(\phi_{i,j+1}^n + \phi_{i,j}^n - \phi_{i-1,j+1}^{n+1} - \phi_{i-1,j}^{n+1} - \phi_{i-1,j+1}^n - \phi_{i-1,j}^n)$$

At the top boundary, $j = \text{JMAX}$,

$$(\phi_y)_{i-1/2,j-1/2}^{n+1/2} + a_{i-1/2,j-1/2}(\phi_x)_{i-1/2,j-1/2}^{n+1/2} = 0 \qquad (C10)$$

is used, where

$$a_{i-1/2,j-1/2} = \frac{(BD)_{i-1/2,j-1/2}}{A}$$

$$B_{i-1/2,j-1/2} = \frac{1 - M_\infty^2}{\delta^{2/3}} - M_\infty^2 \frac{(\gamma^* + 1)}{2}(\phi_{i,j}^n - \phi_{i-1,j}^n + \phi_{i,j-1}^n - \phi_{i-1,j-1}^n)$$

The tridiagonal coefficients are

$$A_j = \frac{a_{i-1/2,j-1/2}}{x_i - x_{i-1}} - \frac{1}{y_j - y_{j-1}}$$

$$B_j = \frac{a_{i-1/2,j-1/2}}{x_i - x_{i-1}} + \frac{1}{y_j - y_{j-1}}$$

$$C_j = 0$$

$$D_j = -\frac{\phi_{i-1,j}^{n+1} + \phi_{i-1,j}^n + \phi_{i,j}^n - \phi_{i-1,j-1}^{n+1} - \phi_{i-1,j-1}^n - \phi_{i,j-1}^n}{y_j - y_{j-1}}$$

$$- \frac{a_{i-1/2,j-1/2}}{x_i - x_{i-1}}(\phi_{i,j-1}^n + \phi_{i,j}^n - \phi_{i-1,j-1}^{n+1} - \phi_{i-1,j}^{n+1} - \phi_{i-1,j-1}^n - \phi_{i-1,j}^n)$$

At the point $(i,j) = (2,1)$

$$(\phi_y)_{i,j+1}^{n+1/2} - a_{i,j+1}(\phi_x)_{i,j+1}^{n+1/2} = 0 \qquad (C11)$$

where ϕ_x and ϕ_y were approximated with backward differences, and in the definition of $a_{i,j+1}$

18

$$B_{i,j+1} = \frac{1 - M_\infty^2}{\delta^{2/3}} - M_\infty^2(\gamma^* + 1)\frac{\phi_{i+1,j+1}^n - \phi_{i-1,j+1}^n}{x_{i+1} - x_{i-1}}$$

The difference equation for (C11) is

$$\frac{\phi_{i,j+1}^{n+1} - \phi_{i,j}^{n+1} + \phi_{i,j+1}^n - \phi_{i,j}^n}{y_{j+1} - y_j} - a_{i,j+1}\frac{\phi_{i,j+1}^{n+1} - \phi_{i-1,j+1}^{n+1} + \phi_{i,j+1}^n - \phi_{i-1,j+1}^n}{x_i - x_{i-1}} \qquad (C12)$$

Using the upstream boundary condition

$$(\phi_t)_{i-1/2,j+1}^{n+1/2} - b_{i-1/2,j+1}(\phi_x)_{i-1/2,j+1}^{n+1/2} = 0$$

the relationship

$$\phi_{i-1,j+1}^{n+1} = \phi_{i,j+1}^n + (1 + \frac{b_{i-1/2,j+1}\Delta t}{x_i - x_{i-1}})^{-1}(1 - \frac{b_{i-1/2,j+1}\Delta t}{x_i - x_{i-1}})(\phi_{i-1,j+1}^n - \phi_{i,j+1}^{n+1})$$

was substituted in (C12). The tridiagonal coefficients at $(i,j) = (2,1)$ then became

$$A_j = 0$$

$$B_j = -\frac{1}{y_{j+1} - y_j}$$

$$C_j = \frac{1}{y_{j+1} - y_j} - \frac{a_{i,j+1}}{x_i - x_{i-1}}\lfloor 1 + (1 + \frac{b_{i-1/2,j+1}\Delta t}{x_i - x_{i-1}})^{-1}(1 - \frac{b_{i-1/2,j+1}\Delta t}{x_i - x_{i-1}})\rfloor$$

$$D_j = -\frac{a_{i,j+1}}{x_i - x_{i-1}}\lfloor 1 + (1 + \frac{b_{i-1/2,j+1}\Delta t}{x_i - x_{i-1}})^{-1}(1 - \frac{b_{i-1/2,j+1}\Delta t}{x_i - x_{i-1}})\rfloor\phi_{i-1,j+1}^n$$

$$- \frac{\phi_{i,j+1}^n - \phi_{i,j}^n}{y_{j+1} - y_j}$$

At $(i,j) = (2,JMAX)$,

$$(\phi_y)_{i,j-1}^{n+1/2} + a_{i,j-1}(\phi_x)_{i,j-1}^{n+1/2} = 0 \qquad (C13)$$

where ϕ_x and ϕ_y were approximated with backward and forward differences, respectively, and in $a_{i,j-1}$

$$B_{i,j-1} = \frac{1 - M_\infty^2}{\delta^{2/3}} - M_\infty^2(\gamma* + 1)\frac{\phi_{i+1,j-1}^n - \phi_{i-1,j-1}^n}{x_{i+1} - x_{i-1}}$$

Combining (C13) and the upstream condition

$$(\phi_t)_{i-1/2,j-1}^{n+1/2} + b_{i-1/2,j-1} \, (\phi_x)_{i-1/2,j-1}^{n+1/2}$$

The tridiagonal coefficients became

$$A_j = -\frac{1}{y_j - y_{j-1}} + \frac{a_{i,j-1}}{x_i - x_{i-1}} \left[1 + (1 + \frac{b_{i-1/2,j-1}\Delta t}{x_i - x_{i-1}})^{-1}(1 - \frac{b_{i-1/2,j-1}\Delta t}{x_i - x_{i-1}})\right]$$

$$B_j = \frac{1}{y_j - y_{j-1}}$$

$$C_j = 0$$

$$D_j = \frac{a_{i,j-1}}{x_i - x_{i-1}} \left[1 + (1 + \frac{b_{i-1/2,j-1}\Delta t}{x_i - x_{i-1}})^{-1}(1 - \frac{b_{i-1/2,j-1}\Delta t}{x_i - x_{i-1}})\right]\phi_{i-1,j-1}^n$$

$$- \frac{\phi_{i,j}^n - \phi_{i,j-1}^n}{y_j - y_{j-1}}$$

20

References

1. Ballhaus, W. F.; and Goorjian, P. M.: Implicit Finite-Difference Computations of Unsteady Transonic Flows about Airfoils, AIAA Journal, Vol. 15, No. 12, Dec. 1977, pp. 1728-1735.

2. Houwink, R.; and van der Vooren, J.: Improved Version of LTRAN2 for Unsteady Transonic Flow Computations, AIAA Journal, Vol. 18, No. 8, August 1980, pp. 1008-1010.

3. Hessenius, K. A.; and Goorjian, P. M.: Validation of LTRAN2-HI by Comparison with Unsteady Transonic Experiment, AIAA Journal, Vol. 20, No. 5, May 1982, pp. 731-732.

4. Murman, E. M.: Analysis of Embedded Shock Waves Calculated by Relaxation Methods, Proceedings of AIAA Computational Fluid Dynamics Conference, July 1973, pp. 27-40.

5. Engquist, B. E.; and Osher, S. J.: Stable and Entropy Satisfying Approximations for Transonic Flow Calculations, Mathematics of Computation, Vol. 34, No. 149, January 1980, pp. 45-75.

6. Goorjian, P. M.; and Van Buskirk, R.: Implicit Calculations of Transonic Flow Using Monotone Methods, AIAA Paper 81-0331, January 1981.

7. Edwards, J. W.; Bennett, R. M.; Whitlow, W., Jr.; and Seidel, D. A.: Time-Marching Transonic Flutter Solutions Incuding Angle-of-Attack Effects, AIAA Paper 82-0685, May 1982.

8. Seidel, D. A.; Bennett, R. M.; and Whitlow, W., Jr.: An Exploratory Study of Finite Difference Grids for Transonic Unsteady Aerodynamics, AIAA Paper 83-0503, January 1983.

9. Ballhaus, W. F.; and Steger, J. L.: Implicit Approximate Factorization Schemes for the Low-Frequency Transonic Equation, NASA TM X-73,082, Nov. 1975.

10. Jameson, A.: Transonic Flow Calculations, Lectures presented at the Von Karman Institute, Rhode-St-Genese, Belgium, March 1976.

11. Rizzetta, D. P.; and Chin, W. C.: Effect of Frequency in Unsteady Transonic Flow, AIAA Journal, Vol. 17, No. 7, July 1979, pp. 779-781.

12. Kwak, D.: Nonreflecting Far-Field Boundary Conditions for Unsteady Transonic Flow Computation, AIAA Journal, Vol. 19, No. 11, Nov. 1981, pp. 1401-1407.

13. Engquist, B.; and Majda, A.: Numerical Radiation Boundary Conditions for Unsteady Transonic Flow, Journal of Computational Physics, Vol. 40, 1981, pp. 91-103.

14. Bayliss, A.; and Turkel, E.: Far Field Boundary Conditions for Compressible Flows, NASA CP-2201, 1982, pp. 1-19.

15. Bland, S. R.: Development of Low-Frequency Kernel-Function Aerodynamics for Comparison with Time-Dependent Finite-Difference Methods, NASA TM 83283, May 1982.
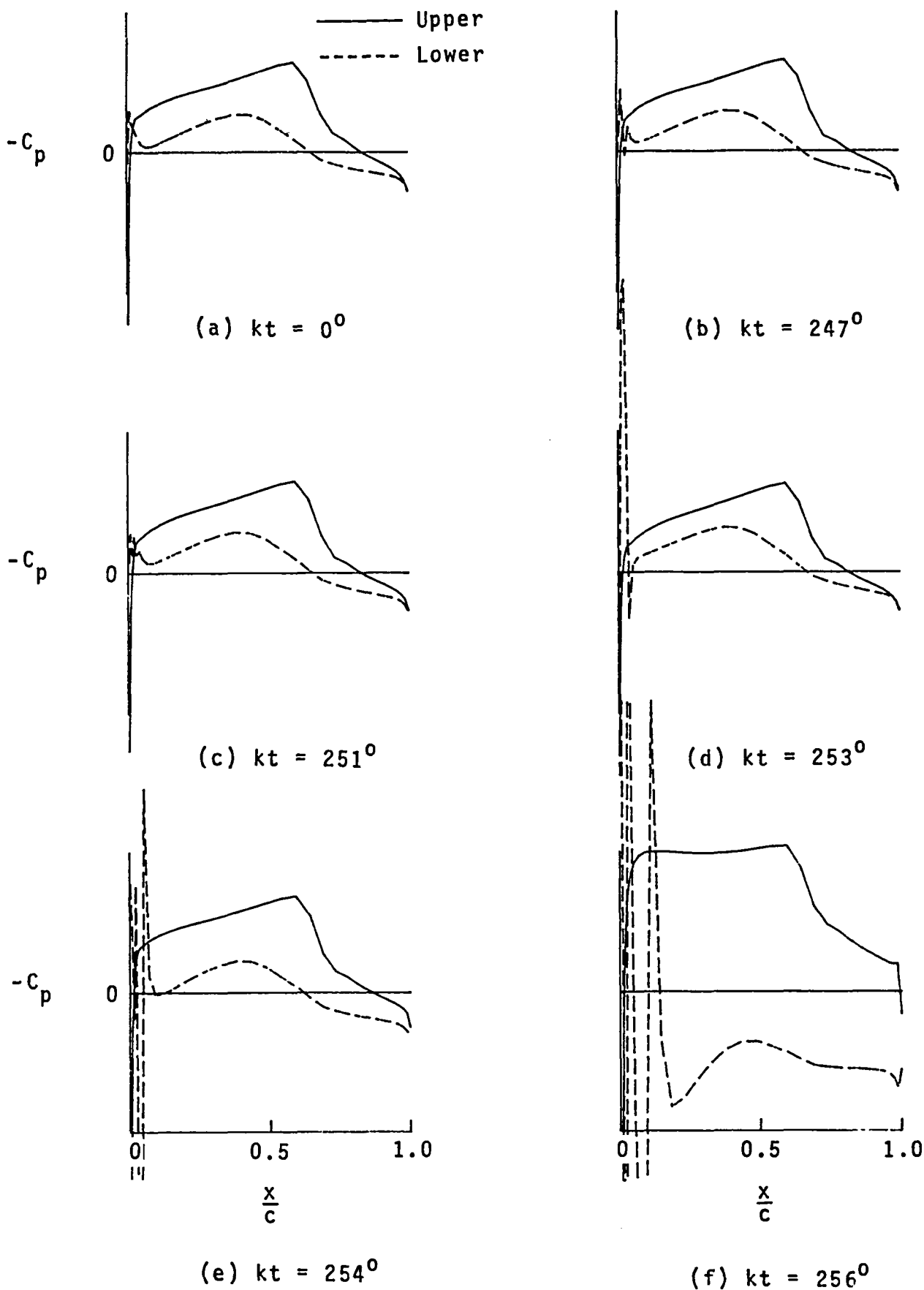
Figure 1. Unsteady pressure distributions on a pitching MBB-A3 airfoil, $M_\infty = 0.8$, k = 0.2, Murman-Cole differencing.
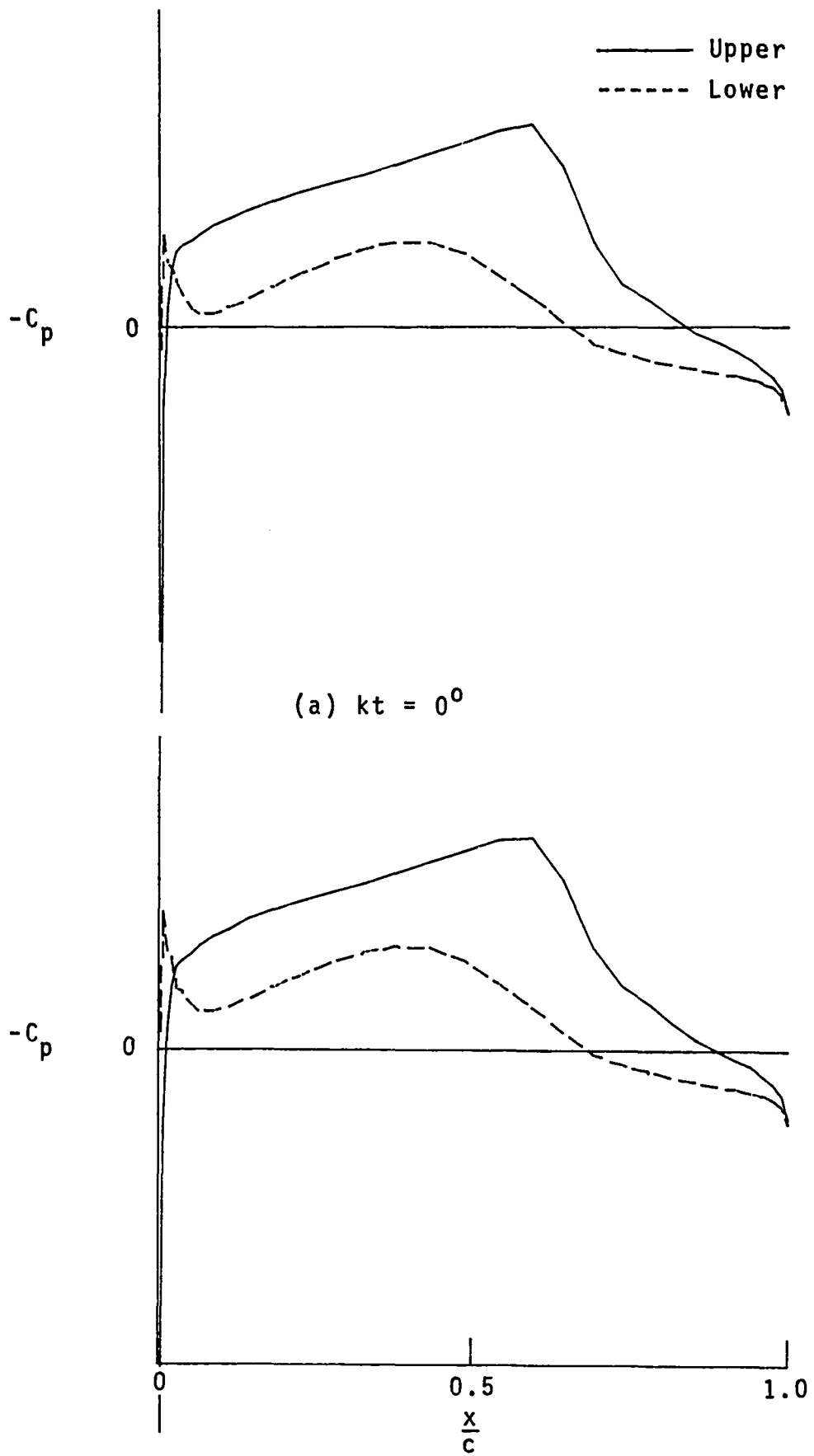
(a) kt = 0°

(b) kt = 1080°

Figure 2. Unsteady pressure distributions on a pitching MBB-A3 airfoil, $M_\infty = 0.8$, k = 0.2, Engquist-Osher differencing.
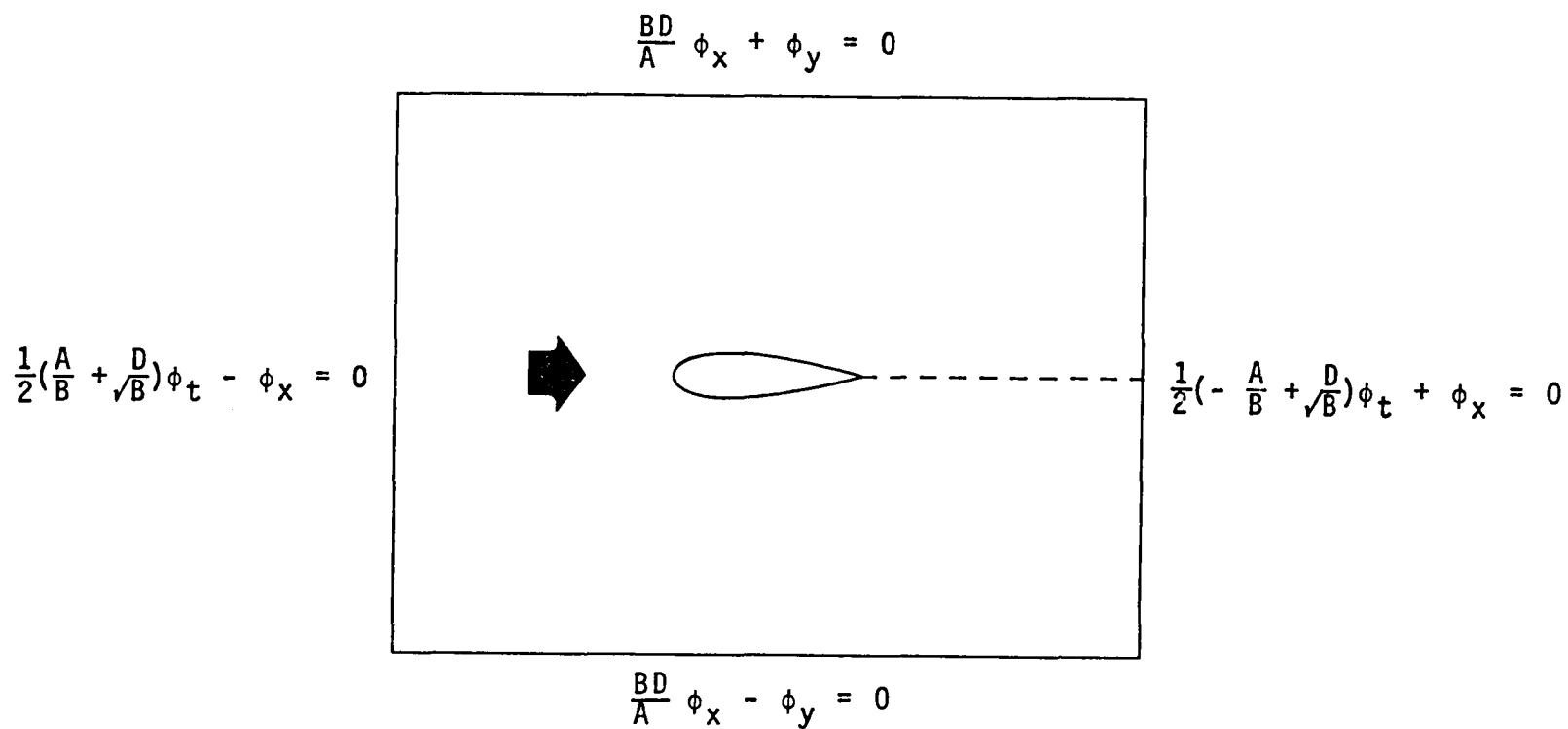
$$\frac{BD}{A} \phi_x + \phi_y = 0$$

$$\frac{1}{2}(\frac{A}{B} + \frac{D}{\sqrt{B}})\phi_t - \phi_x = 0$$

$$\frac{1}{2}(- \frac{A}{B} + \frac{D}{\sqrt{B}})\phi_t + \phi_x = 0$$

$$\frac{BD}{A} \phi_x - \phi_y = 0$$

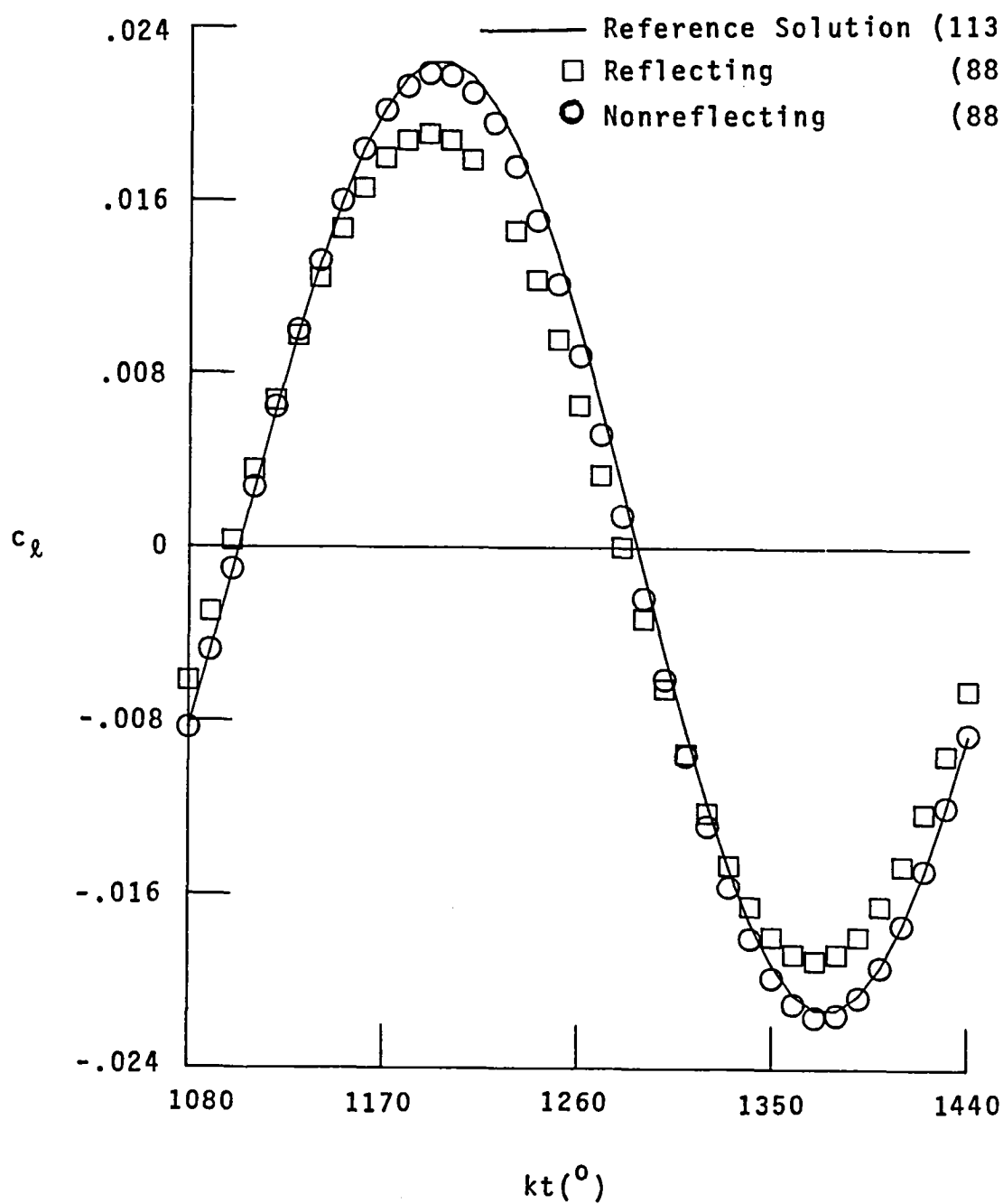Figure 3. Nonreflecting far-field boundary conditions.

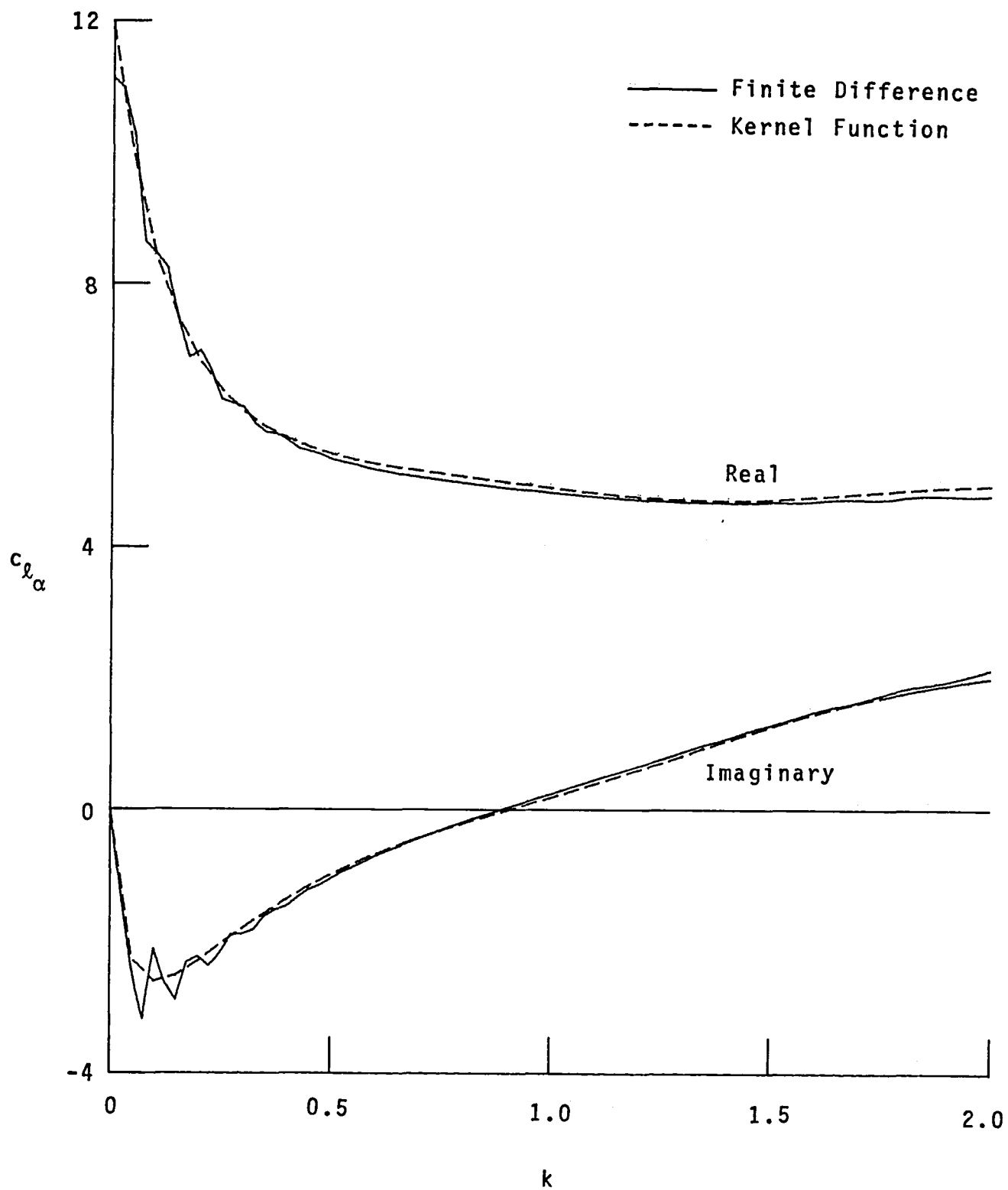Figure 4.   Unsteady lift coefficient for an NACA 64A010 airfoil, $M_\infty = 0.825$, $k = 0.5$.

Figure 5a. Force response with reflecting far-field boundary conditions for a flat plate airfoil, $M_\infty = 0.85$.
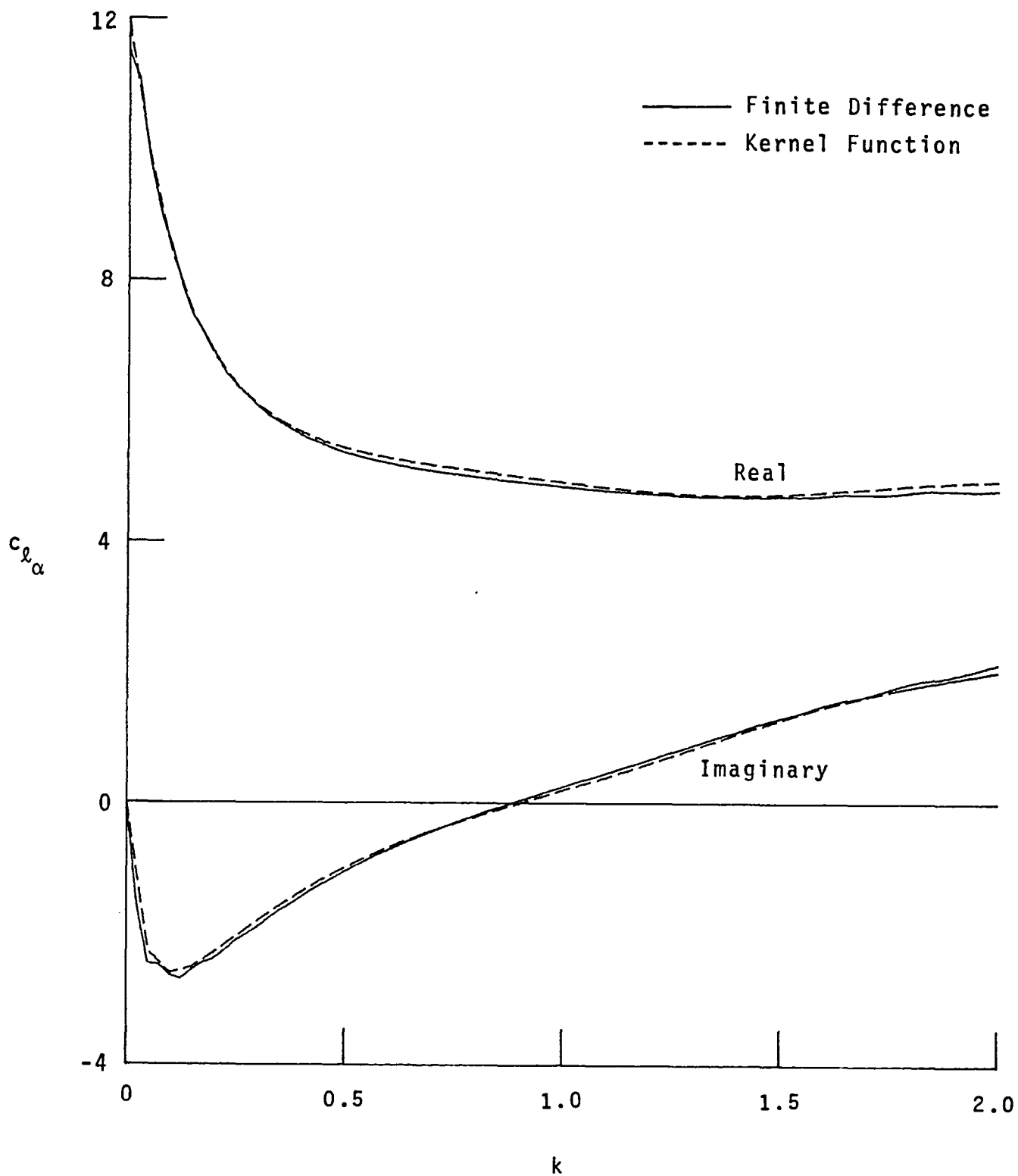
Figure 5b. Force response with nonreflecting far-field boundary
conditions for a flat plate airfoil, $M_\infty = 0.85$.

1. Report No. NASA TM-85723	2. Government Accession No.	3. Recipient's Catalog No.
4. Title and Subtitle XTRAN2L: A Program for Solving the General-Frequency Unsteady Transonic Small Disturbance Equation		5. Report Date November 1983
		6. Performing Organization Code 505-33-43-09
7. Author(s) Woodrow Whitlow, Jr.		8. Performing Organization Report No.
		10. Work Unit No.
9. Performing Organization Name and Address NASA Langley Research Center Hampton, VA 23665		11. Contract or Grant No.
		13. Type of Report and Period Covered Technical Memorandum
12. Sponsoring Agency Name and Address National Aeronautics and Space Administration Washington DC 20546		14. Sponsoring Agency Code

15. Supplementary Notes

16. Abstract

A program, XTRAN2L, for solving the general-frequency unsteady transonic small disturbance potential equation has been developed. It is a modification of the LTRAN2-NLR code. The alternating-direction-implicit (ADI) method of Rizzetta and Chin is used to advance solutions of the potential equation in time. Engquist-Osher monotone spatial differencing is used in the ADI solution algorithm. As a result, the XTRAN2L code is more robust and more efficient than similar codes that use Murman-Cole type-dependent spatial differencing. Nonreflecting boundary conditions that are consistent with the general-frequency equation have been developed and implemented at the far-field boundaries. Use of those conditions allow the computational boundaries to be moved closer to the airfoil with no loss of accuracy. This makes the XTRAN2L code more economical to use.

17. Key Words (Suggested by Author(s)) Transonic Unsteady Aerodynamics Transonic Small Disturbance Equation Time Marching Transonic Solutions Monotone Differencing Methods Nonreflecting Boundary Conditions	18. Distribution Statement Unclassified - Unlimited Subject Category - 02

19. Security Classif. (of this report) Unclassified	20. Security Classif. (of this page) Unclassified	21. No. of Pages 28	22. Price A03